Original Article

Institution of MECHANICAL ENGINEERS

Journal of SYSTEMS AND CONTROL ENGINEERING

Proc IMechE Part I:
J Systems and Control Engineering
2015, Vol. 229(3) 235–249

DOI: 10.1177/0959651814559759
pii.sagepub.com
SAGE

Estimation and predictive control of nonlinear diffusion processes with application to drying of coatings

Xiaoqing Cao and Beshah Ayalew

Abstract

This article deals with the estimation and control of a class of distributed parameter processes dominated by nonlinear diffusion. The major challenges in control of such systems lie in the nonlinear infinite-dimensional nature of the systems and the lack of direct sensing for relevant system states. In the proposed scheme, the proper orthogonal decomposition-Galerkin method is adopted to derive a reduced-order model in terms of temporal coefficients from the original system described by nonlinear partial differential equation(s). To overcome the sensing problem, the unscented Kalman filter is implemented to estimate the temporal coefficients of the reduced-order model online and subsequently reconstruct the distributed system states. A set of improved sufficient conditions are also established to ensure stability of the estimation scheme. Then, once these difficulties are addressed, a nonlinear model predictive control scheme is formulated to achieve desired control objectives such as trajectory tracking for distributed states, energy optimization and quality control. The proposed estimation and control scheme is demonstrated via an application to infrared drying of coatings in the automotive industry.

Keywords

Nonlinear diffusion process, proper orthogonal decomposition, proper orthogonal decomposition-Galerkin method, unscented Kalman filter, model predictive control, drying process

Date received: 14 January 2014; accepted: 14 October 2014

Introduction

Many industrial processes are modelled as distributed parameter systems (DPSs) where the states, inputs and/or outputs evolve both in space and in time. Among the different kinds of DPSs, the convection-diffusion-reaction processes, which are modelled by parabolic partial differential equations (PDEs), are of particular industrial importance.[1] The design of control schemes for these DPSs is much more complex than that of lumped parameter systems (LPSs) due to the infinite dimensionality of the DPSs. As such, the field of control design for DPSs has received considerable attention since the 1960s[2] particularly for its theoretical richness. In practice, however, the implementable control solutions for parabolic PDEs usually start with some model reduction to a finite-dimensional description. This is because of the physical limitations of available sensors and actuators as well as the finite limits on digital control and computation resources.[3]

For linear or quasi-linear parabolic PDEs, a standard way to derive the reduced-order model (ROM) is to use eigenfunction expansion[4] combined with the Galerkin method.[1,5] This linear model reduction approach exploits the fact that the spectrum of spatial differential operators for parabolic PDEs can be separated into two parts: an infinite number of fast modes and a finite number of slow modes.[6] The dominant dynamics of the system can then be approximated by a finite number of ordinary differential equations (ODEs) derived from the slow modes using Galerkin projection.[7,8] However, the complete neglect of the fast modes may cause accuracy issues because of information loss. To compensate for the neglected fast modes and to improve the accuracy of the reduced model, nonlinear model reduction methods, such as inertial manifolds

Clemson University International Center for Automotive Research (CU-ICAR), Greenville, SC, USA

Corresponding author:
Xiaoqing Cao, Clemson University International Center for Automotive Research (CU-ICAR), 4 Research Drive, Greenville, SC 29607, USA.
Email: xiaoqin@g.clemson.edu

(IM)[6,9] and approximate inertial manifolds (AIM),[10–12] are often used to obtain ROMs for linear and quasi-linear PDEs.

However, some practical DPSs are inherently nonlinear due to system characteristics like nonlinear diffusivity[7,13,14] or input nonlinearity.[15] With nonlinear differential operators in the system PDEs, it is often difficult, if not impossible, to derive the IM or AIM analytically. Fortunately, it turns out that the so-called pseudo-modal method is a good alternative for model reduction for such PDEs.[1] This method works as an extension of the eigenfunction expansion method where it is possible to choose a set of known basis functions and to use them to reduce nonlinear PDE systems. In this regard, proper orthogonal decomposition (POD) is an effective way to find an optimal set of basis functions that captures the dominant spatial dynamics of the PDE system from available system measurements (called snapshots).[16–19] The basis functions can be incorporated into some weighted residual method, such as Galerkin projection, to derive ROMs thereby changing the nonlinear PDE to a finite system of nonlinear ODEs. However, one critical problem of implementing this POD-Galerkin method is the very availability of snapshots for spatially distributed states. At some practical level, this problem may be solved if some high-resolution simulations of the original PDE system model can be used along with available measurements, if any.[7] This latter approach has been successfully applied in some works.[20–22]

As far as suitable control strategies to apply, several methods have been proposed for control of linear or semi-linear PDE systems. These include classical approaches such as finite-dimensional state/output feedback control based on reduced-order ODE models[7,8] or more recent ones such as backstepping boundary control of linear PDEs without model reduction.[23] Control of PDE models with nonlinearities in the diffusion term is rarely addressed. A related work is the one in Xu et al.[24,25] which addressed bilinear quadratic control of parabolic PDEs with diffusivity actuation, where the control input multiplies the diffusion term, which is otherwise linear. In this work, we address systems with strongly nonlinear diffusion terms that do not necessarily contain the control input.

Furthermore, we seek to incorporate explicit process constraints and address multiple objectives in the control design. In this regard, model predictive control (MPC)[26–28] has emerged as a popular framework for its ability to handle hard process constraints and to formulate the control problem as a constrained optimization with multiple objectives. In MPC, the process dynamics (linear or nonlinear) can be treated as constraints of the optimization, while the multiple control objectives, which are often encountered in industrial processes, are enforced by a set of properly defined objective functions. In Padhiyar and Bhartiya,[29] lexicographic optimization–based MPC was proposed for profile control of plug flow reactors. The controller utilizes lexicographic optimization to prioritize different sections of the profile in case the target profile is unachievable. A similar control strategy using linear MPC can be found in Vada et al.[30] To incorporate nonlinear PDE systems into linear MPC frameworks, one possible approach is to linearize the nonlinear PDE at nominal operating points and design the controller based on the linearized model.[1,14,31] Dufour et al.[14,31,32] proposed a two-level optimization scheme that uses this approach for infrared-convective drying of a paint film. The nonlinear PDE of the drying process is first linearized around a predefined operating point. Then, the linear model is used to find the optimal input variations with online predictive control. However, such linear models are valid only in a small neighbourhood of the pre-selected operating points. Some of the problems with this local approximation can be avoided by using extensions of the modal decomposition techniques mentioned above, where the linear or nonlinear PDE models are first transformed into finite-dimensional ODE models. Then, linear MPC or nonlinear MPC (NMPC) can be readily devised based on these ODE models. Examples of successful investigations that use this latter framework can be found in previous studies.[33–36]

The lack of feasible sensors for measuring the spatially distributed states is also a common challenge in implementing NMPC schemes for DPSs. In general, only selected system outputs can be measured in parts of the spatial domain, often on a boundary of the domain. This means that the full state must be reconstructed from the limited output information by designing full state observers, most often based on ROMs. For linear or semi-linear DPSs, the observers are usually designed in analogy to those for LPSs. This includes high-order Kalman filters[20] and high-order sliding mode observers.[37,38] For a more complete review of observers for linear DPSs, see Hidayat et al.[39] and references therein. For nonlinear DPSs, the extended Kalman filter (EKF) is a widely used nonlinear filtering strategy.[40] Similar to the linearization-based MPC, the required local (Jacobian) linearization step in the EKF only preserves first-order accuracy, which might not be acceptable for high performance control of nonlinear DPSs. To address this limitation, the unscented Kalman filter (UKF) has been proposed to accurately estimate the states of nonlinear systems.[41–43] By using the unscented transformation (UT) instead of local linearization, the UKF is reported to offer higher accuracy (up to second order) at a similar computational cost as the EKF.[44–46] Applications given in previous studies[47–49] demonstrate the effectiveness of the UKF to estimate the full state of nonlinear systems.

This work is motivated by the potential of the POD-Galerkin technique for nonlinear PDE model reduction and of the UKF for nonlinear state estimation. First, we give a detailed derivation of the POD-Galerkin technique for a general parabolic PDE system with nonlinear diffusivity. The UKF is then constructed

based on the POD-Galerkin ROM, where the temporal coefficients are estimated as states, given some partial measurements. Finally, with the available POD basis functions and the estimated temporal coefficients, the spatially distributed system states can be reconstructed. NMPC is then applied under the framework of constrained optimization with multiple objectives. An analytical proof is also included for additional sufficient conditions proposed here for convergent state estimation with UKF.

To illustrate the main points, the process of infrared drying of automotive coatings, which is dominated by nonlinear diffusivity, is used as a case study. The complete thin-film drying process model consists of a coupled system of a nonlinear parabolic PDE and an ODE, which govern the evolution of moisture content and temperature, respectively. In this application, the distributed system states (moisture content across film depth) cannot be measured directly and need to be estimated online from available measurements. Other similar applications to which the proposed scheme could apply include thermal chemical vapour deposition[7,50] and curing process in semiconductor packaging.[13]

The rest of this article is organized as follows: In section 'Proposed control scheme', the proposed estimation and control scheme is outlined briefly, and in section 'POD-Galerkin model reduction', the POD-Galerkin model reduction is detailed for a parabolic PDE processes with nonlinear diffusivity. Section 'UKF' introduces the implementation of UKF-based estimation for these processes. Section 'Case study' provides a case study on the drying process of automotive coatings. It includes details of a NMPC scheme that builds on the preceding discussions, as well as simulation results that illustrate the efficacy of the model reduction and estimation schemes. Conclusions are included in section 'Conclusion'.

Proposed control scheme

General one-dimensional parabolic PDE system with nonlinear diffusivity

As already pointed out, many industrial processes are dominated by convection-diffusion-reaction phenomena.[51] In particular, diffusion is often state dependent, thereby contributing to the main nonlinearity of the process. A general one-dimensional (1D) model for such a process is given by

$$\frac{\partial X}{\partial t} = \frac{\partial}{\partial z}\left[f(X,t)\frac{\partial X}{\partial z}\right] + g(X,u,z,t) \tag{1}$$

with boundary conditions defined by

$$A_1(z,t)X + B_1(z,t)\frac{\partial X}{\partial z} = C_1(z,t), \quad \text{at } z = z_1 \tag{2}$$

$$A_2(z,t)X + B_2(z,t)\frac{\partial X}{\partial z} = C_2(z,t), \quad \text{at } z = z_2 \tag{3}$$

and initial condition

$$X(z,t_0) = X_0(z) \tag{4}$$

where $X(z,t)$ denotes the process state variables such as temperature, concentration or moisture content, which are distributed in spatial domain $z \in [z_1, z_2]$ with time $t \in [t_0, +\infty)$. The nonlinear diffusion coefficient $f(X,t)$ is a function of state variable X and time t. $g(X,u,z,t)$ is a general nonlinear function which could be a source term that enters the PDE in an additive fashion. $u = [u_1 \ldots u_k]^T$ is the system input vector. The specific functions A_1, B_1, C_1 and A_2, B_2, C_2 take on different forms depending on the type of the prevailing boundary conditions.

It is worthy to point out that the nonlinear parabolic PDE system described above may often be coupled with some nonlinear ODEs for lumped parameter dynamics. This coupled PDE-ODE system can be treated as one ODE system once the ROM is obtained for PDE system. In section 'Case study', we illustrate how the above model structure arises using the infrared drying process as an example.

UKF-based POD-NMPC scheme

In this article, the scheme shown in Figure 1 is proposed for the control of nonlinear parabolic systems described above. This UKF-based POD-NMPC scheme is implemented as follows: from the initial snapshot of the plant, a set of problem-oriented POD basis functions are calculated. With the POD-Galerkin method, the original PDE is reduced to nonlinear ODEs in terms of the temporal coefficients as the states. The UKF is then applied to estimate these temporal coefficients based on the reduced ODE model and available measurements. Then, with the reconstructed original system states, a constrained optimization problem is formulated and solved iteratively to minimize the predefined objective/cost functions in a NMPC framework.

In the following sections, each of the main blocks of the scheme in Figure 1 is discussed in further detail assuming the nonlinear PDE model given in equation (1) for the nonlinear process.

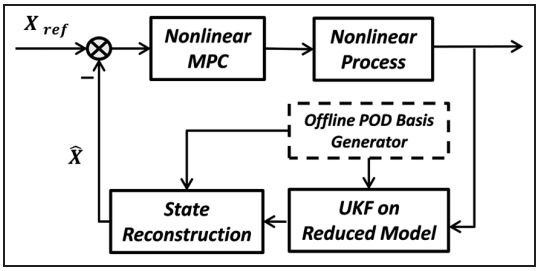

Figure 1. UKF-based POD-NMPC scheme.

POD-Galerkin model reduction

POD

POD is a powerful model reduction method for high-dimensional systems.[52,53] It is also known as principal component analysis, Karhunen–Loeve decomposition and singular value decomposition (SVD).[54] The basic idea of this method is to generate a set of independent basis functions from simulated or experimental data. The state variable is sought to be approximated in the following form

$$X(z,t) \cong \hat{X}(z,t) = \sum_{k=1}^{N} a_k(t)\varphi_k(z) \tag{5}$$

For convenience of practical implementation, both spatial and temporal discretizations are adopted. Consider a given set of sampled data (snapshot): $\chi = [\chi_1, \ldots, \chi_m]$ and $\chi_i \in \mathbb{R}^n\,(i = 1, \ldots, m)$, where $n \in \mathbb{R}$ is the size of spatial discretization and $m \in \mathbb{R}$ is the size of temporal discretization. The objective of POD is to obtain a reduced N-dimensional subspace $V_{sub} \in \mathbb{R}^n$, such that the linear combination of the basis vectors from this subspace can approximate the original sampled data χ optimally, in the least-square sense.[16] Let $V_{sub} = \text{span}\{\tilde{\varphi}_1, \ldots, \tilde{\varphi}_N\}$, the problem can be transformed into one of finding orthogonal basis vectors $\tilde{\varphi}_i\,(i = 1, \ldots, N)$, such that the following error is minimized[24,25]

$$\text{Min}\ \frac{1}{m}\sum_{i=1}^{m}\left\|\chi_i - \sum_{k=1}^{N}(\chi_i, \tilde{\varphi}_k)\tilde{\varphi}_k\right\|^2 \tag{6}$$

where $(\cdot, \cdot)$ denotes the standard $\mathcal{L}^2$ inner product and $\|x\|^2 = \sqrt{x^T x}$. The POD basis vectors satisfy orthogonality

$$(\tilde{\varphi}_i, \tilde{\varphi}_j) = \delta_{ij} \tag{7}$$

$\delta_{ij}\,(i, j = 1, \ldots, N)$ is the commonly defined Kronecker delta function. The solution of equation (6) can be found by defining a correlation matrix between χ_i and $\chi_j (i, j = 1, \ldots, m)$ and deriving the POD basis vectors from the resulting eigenvalue problems.[16,18,55] A more practical way to extract POD basis vectors from sampled data is to use SVD.[16,18,56] Applying SVD to the snapshot $\chi \in \mathbb{R}^{n*m}$, we have

$$\chi = U\Sigma V^* \tag{8}$$

where $U \in \mathbb{R}^{n*n}$ and $V \in \mathbb{R}^{m*m}$ are orthogonal unitary matrices, and $\Sigma = \begin{pmatrix} \Sigma_r & 0 \\ 0 & 0 \end{pmatrix} \in \mathbb{R}^{n*m}$ and $\Sigma_r = \text{diag}(\sigma_1, \ldots, \sigma_r)$. $\sigma_i (k = 1, \ldots, r)$ are the singular values of matrix χ and are arranged in the order $\sigma_1 \geqslant \sigma_2 \geqslant \cdots \geqslant \sigma_r$. Then, the first r columns of U are the orthogonal POD basis vectors $(\tilde{\varphi}_1, \ldots, \tilde{\varphi}_r)$. The POD basis functions $\varphi_k(z)\,(k = 1, \ldots, r)$ can be obtained by interpolation from the corresponding $\tilde{\varphi}_k$. Then, the spatial distribution of the state variables can be approximated by the first L POD basis functions $X(z,t) \cong \sum_{k=1}^{L} a_k(t)\varphi_k(z)$ with the approximation accuracy given by

$$A(L) = \frac{\sum_{i=1}^{L}\sigma_i^2}{\sum_{j=1}^{r}\sigma_j^2} \tag{9}$$

Once the spatial variation is approximated, Galerkin projection can be applied to obtain the reduced-order ODE model, which represents the dynamics of temporal coefficients $a_k(t)$. This is briefly outlined next.

Galerkin method

The Galerkin projection is a kind of weighted residual method which can be used to determine the temporal coefficient $a_k(t)$ via pseudo-modal analysis.[1] We first write the approximated solution as follows

$$\hat{X}(z,t) = \sum_{k=1}^{L} a_k(t)\varphi_k(z) \tag{10}$$

Once the basis functions $\varphi_k(z)\ (k = 1, \ldots, L)$ are derived, coefficients $a_k(t)$ can be determined by the method of weighted residuals. The idea is to determine $a_k(t)$ such that the residual

$$R_e(z,t) = \frac{\partial \hat{X}}{\partial t} - \frac{\partial}{\partial z}\left[f(\hat{X},t)\frac{\partial \hat{X}}{\partial z}\right] - g(\hat{X}, u, z, t) \tag{11}$$

is small under the criterion that the weighted residual vanishes

$$\int \omega_k \cdot R_e(z,t)dz = 0 \quad (k = 1, \ldots, L) \tag{12}$$

Different choices of the weighting functions ω_k lead to different weighted residual methods. In the Galerkin method, the weighting functions are selected to be the basis functions themselves. That is

$$\int \varphi_k(z) \cdot R_e(z,t)dz = 0 \quad (k = 1, \ldots, L) \tag{13}$$

Then, by substituting the orthogonality as well as the corresponding boundary conditions, the ROM in nonlinear state-space form can be described as follows

$$\begin{cases} \dot{a}(t) = \mathcal{F}(a(t), \varphi(z),\ t) \\ \hat{X}(z,t) = \varphi^T(z)a(t) \end{cases} \tag{14}$$

with $a(t) = [a_1(t), \ldots, a_L(t)]^T$ and $\varphi(z) = [\varphi_1(z), \ldots, \varphi_L(z)]^T$. $\mathcal{F}$ is the resulting nonlinear function characterizing the coupled dynamics of temporal coefficients in the POD approximation, and an example is given in section 'Case study'. The initial value of the temporal coefficients can be obtained from $a_k(0) = \int X(z,0)\varphi_k(z)dz$.

UKF

In this section, the practical implementation of the UKF on a discrete nonlinear system is reviewed. A set of modified sufficient condition for stability of the UKF and the proof of the theorem are provided in Appendix 1.

Extended from the most commonly used nonlinear filtering technique of the EKF, the UKF has been recently proposed to estimate the states of nonlinear systems.[42,44] The UKF shares the same prediction–correction structure as the classical linear Kalman filter and the EKF. In these two steps, covariance matrices of both the predicted and corrected variables are calculated. Instead of the Jacobian linearization used in the EKF, the so-called UT is applied in the UKF. For a vector random variable x, the UT is proposed to predict the mean and covariance of vector random variable y, which is related to x through a nonlinear function

$$y = \mathcal{F}(x) \tag{15}$$

This is achieved by defining a set of sigma points which capture the mean and covariance of initial vector random variable x and propagate them through nonlinear function $\mathcal{F}$ that serves as the UT. Analysis of the output of the nonlinear function $\mathcal{F}$ generates the predicted mean and covariance to second-order accuracy.

For a practical implementation, the UKF is often described in discrete time. Assume the nonlinear system, such as equation (14), is already discretized using conventional methods and put in the form

$$x_k = \mathcal{F}_d(x_{k-1}) + q_k \tag{16}$$

$$\zeta_k = H_k x_k + r_k \tag{17}$$

where x_k is the n-dimensional state variable (in the present case, the temporal coefficients of the POD) and ζ_k is the m-dimensional system output. $\mathcal{F}_d$ is the discretized nonlinear system function and H_k is the output matrix. q_k and r_k are process noise and output noise with covariance matrices Q_k and R_k, respectively, and k stands for time index. Assume at time $k-1$, state estimation is $\hat{x}_{k-1}$ with the covariance $\hat{P}_{k-1}$. The UKF implementation steps are summarized below:[42,57]

Step 1. Generate a set of sigma points $\sigma_i (i = 1, \ldots, n)$ and intermediate variable χ_{k-1}

$$\begin{cases} \chi_{k-1,0} = \hat{x}_{k-1} \\ \chi_{k-1,i} = \hat{x}_{k-1} + \sigma_i \\ \chi_{k-1,i+n} = \hat{x}_{k-1} - \sigma_i \end{cases}$$

where $\sigma_i (i = 1, \ldots, n)$ are the columns from $\sqrt{n\hat{P}_{k-1}}$.

Step 2. Propagate through system state equation and prediction

$$\chi_{k|k-1,j} = \mathcal{F}_d(\chi_{k-1,j}) \quad j = 0, \ldots, 2n$$

with predicted mean and covariance

$$\hat{x}_{k|k-1} = \sum_{j=0}^{2n} \varpi_j \cdot \chi_{k|k-1,j}$$

where $\begin{cases} \varpi_j = \kappa/(n+\kappa) & j = 0 \\ \varpi_j = 1/(2(n+\kappa)) & j = 1, \ldots, 2n \end{cases}$, κ is a constant parameter

$$\hat{P}_{k|k-1} = \sum_{j=0}^{2n} \varpi_j \left(\chi_{k|k-1,j} - \hat{x}_{k|k-1}\right) \left(\chi_{k|k-1,j} - \hat{x}_{k|k-1}\right)^T$$

Step 3. Propagate through the output equation

$$\hat{\zeta}_k = H_k \hat{x}_{k|k-1}$$
$$\hat{P}_{\zeta\zeta} = H_k \hat{P}_{k|k-1} H_k^T + R_k$$
$$\hat{P}_{x\zeta} = \hat{P}_{k|k-1} H_k^T$$

Step 4. Correct the mean and covariance

$$\hat{x}_k = \hat{x}_{k|k-1} + \hat{P}_{x\zeta} \hat{P}_{\zeta\zeta}^{-1} (\zeta_k - \hat{\zeta}_k)$$
$$\hat{P}_k = \hat{P}_{k|k-1} - \hat{P}_{x\zeta} \hat{P}_{\zeta\zeta}^{-1} \hat{P}_{x\zeta}^T$$

This completes a single discrete time step of the UKF estimation. With the new mean and covariance, state estimation proceeds iteratively for the subsequent steps.

Case study

Drying process of automotive coatings

In automotive manufacturing, the paint drying process involves a set of steps designed to impart good corrosion and scratch resistance properties as well as glossy appearances that meet customer expectations. The use of an infrared radiative (IR) heat source is a potential alternative to the convective bake-ovens for its higher energy efficiency, faster response time and better controllability.[58]

A schematic of the drying process setup is shown in Figure 2. Both mass and heat transfer are assumed to take place in the direction perpendicular to the paint surface. As a result, moisture content $\mathcal{M}$ is spatially distributed along the z direction. Moreover, as pointed out in other works,[31,59–61] the temperature difference between the top and bottom layers is negligible since the coating is usually very thin (around 20 μm for basecoat and 100 μm in total[62]). Thus, the temperature of the paint is assumed to be spatially uniform during the drying process.

Infrared drying process constitutes mass and energy transfer phenomenon. The mass transfer equation follows from Fick's law[63]

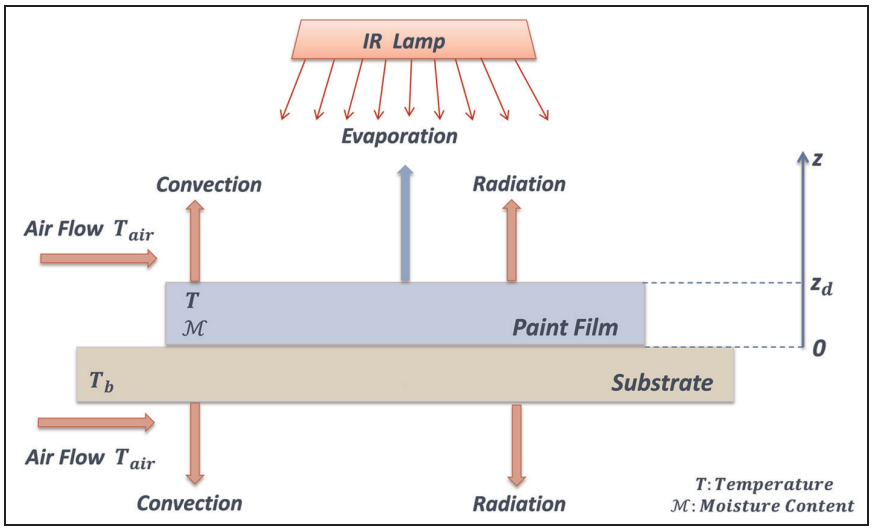

Figure 2. Infrared drying process.

$$\frac{\partial \mathcal{M}}{\partial t} = \frac{\partial}{\partial \xi}\left[D(\mathcal{M}, T)\frac{\partial \mathcal{M}}{\partial \xi}\right] \tag{18}$$

where $\xi \in [0, \xi_d]$ is the space variable in Lagrangian coordinate and is introduced to deal with the shrinkage accompanying the evaporation of water.[31,64] $D(\mathcal{M}, T)$ is the nonlinear diffusion coefficient which depends on the moisture content $\mathcal{M}$ and temperature T, according to

$$D(\mathcal{M}, T) = \frac{D_0 e^{\left(-\frac{a}{\mathcal{M}}\right)} e^{\left(-\frac{E}{RT}\right)}}{(1 + \varepsilon \mathcal{M})^2} \tag{19}$$

where D_0, a, E and R are positive constants and ε is the shrinkage coefficient which depends on the characteristics of the paint material. The two boundary conditions at the top and bottom are

$$-D(\mathcal{M}, T)\frac{\partial \mathcal{M}}{\partial \xi} = \frac{\dot{m}(\bar{\mathcal{M}}, T)}{\rho_d}, \quad \text{at } \xi = \xi_d \tag{20}$$

$$\frac{\partial \mathcal{M}}{\partial \xi} = 0, \quad \text{at } \xi = 0 \tag{21}$$

$\dot{m}(\mathcal{M}, T)$ is the mass transfer rate on the film surface and $\bar{\mathcal{M}}$ is the average moisture content. The expression of $\dot{m}(\mathcal{M}, T)$ is given by the following equation

$$\dot{m}(\bar{\mathcal{M}}, T) = \frac{k_m m_v}{R} p_t \frac{2}{T + T_{air}} \log_{10}\left[\frac{p_t - \mathcal{M}_{air} \cdot p_s(T_{air})}{p_t - a(\bar{\mathcal{M}}) \cdot p_s(T)}\right] \tag{22}$$

where k_m, m_v, p_t and R are positive constants. T and T_{air} are paint temperature and convective air temperature, respectively. $\mathcal{M}_{air}$ is the moisture content in air and $\bar{\mathcal{M}}$ is the average moisture in coatings.[32]

Considering energy transfer under uniform temperature (thin coating) assumption, the energy balance equation can be written as

$$(\rho_p C_p z_p + \rho_s C_s z_s)\frac{dT}{dt} = P_{ab} - P_l - P_{ra} - P_{co} \tag{23}$$

where $P_{ab} = \alpha_{ab} P_{IR}$ is the heat energy absorbed by the paint material, α_{ab} is the IR absorptivity of the paint material and P_{IR} is the heat flux from IR lamp (heat source); $P_l = \mathcal{L}(T)\dot{m}(\bar{\mathcal{M}}, T)$ is the latent heat dissipated with the evaporation of water; $P_{ra} = \sigma_1(T^4 - T_{air}^4) + \sigma_2(T^4 - T_b^4)$ and $P_{co} = h_c(T - T_{air}) + h_c(T - T_b)$ are radiative and convective heat transfer between the paint film and convective air (T_{air}) as well as the substrate and ambient (T_b). Indexes p and s in the left-hand side of equation (22) stand for paint and substrate, respectively. Blanc et al.[65] have shown experimental validation of the above drying model.

It can be seen that, due to the complex and nonlinear dependence of the diffusion coefficient D and the mass transfer rate $\dot{m}$ on the system variables $\mathcal{M}$ and T, the PDE in equation (18) is highly nonlinear. Moreover, it is coupled with the dynamics of the temperature T given by the ODE in equation (23).

POD-Galerkin method for the drying model

We now apply the POD-Galerkin method to the drying model described in the previous section. Assume that the initial set of process snapshots is available, then POD basis functions $\varphi_k(k = 1, \ldots, L)$ with desired accuracy can be calculated. With the POD approximation

$$\hat{\mathcal{M}}(\xi, t) = \sum_{k=1}^{L} a_k(t)\varphi_k(\xi) \tag{24}$$

the residual for the PDE model can be written as

$$R_e(\xi, t) = \frac{\partial \hat{\mathcal{M}}}{\partial t} - \frac{\partial}{\partial \xi}\left[D\left(\hat{\mathcal{M}}, T\right)\frac{\partial \hat{\mathcal{M}}}{\partial \xi}\right] \tag{25}$$

After applying the Galerkin method, we obtain

$$\left(\varphi_j, \frac{\partial \sum_{k=1}^{L} a_k \varphi_k}{\partial t}\right) = \left(\varphi_j, \frac{\partial}{\partial \xi}\left[D\left(\sum_{k=1}^{L} a_k \varphi_k, T\right) \frac{\partial \sum_{k=1}^{L} a_k \varphi_k}{\partial \xi}\right]\right) \quad (26)$$

With the orthogonal property and boundary conditions, the above equation can be simplified into ODEs of the temporal coefficients. Finally, the reduced-order ODE model combining both the dynamics of temporal coefficients and temperature for the drying process is summarized as follows

$$\textit{States}: \begin{cases} \dot{a}_j = \left(\varphi_j \frac{-\dot{m}(\bar{\mathcal{M}}, T)}{\rho_d}\right)|_{\xi_d} - \int_0^{\xi_d} D\left(\sum_{k=1}^{L} a_k \varphi_k, T\right) \frac{\partial \sum_{k=1}^{L} a_k \varphi_k}{\partial \xi} \frac{d\varphi_j}{d\xi}\, d\xi \\ \dot{T} = \frac{1}{(\rho_p C_p z_p + \rho_s C_s z_s)} (\alpha_{ab} P_{IR} - P_l - P_{ra} - P_{co}) \end{cases} \quad (27)$$

$$\textit{Outputs}: \quad Z = \begin{bmatrix} \Gamma \varphi^T a \\ T \end{bmatrix}$$

The first state equation describes the evolution of the j^{th} ($j = 1, \ldots, L$) temporal coefficient corresponding to the j^th POD basis function, and the approximated moisture content can be reconstructed by $\hat{\mathcal{M}} = \varphi^T a$. Initial values of the temporal coefficients can be obtained from $a_k(0) = \int \mathcal{M}(\xi, 0)\varphi_k(\xi)d\xi$. The system input is the heat flux from the IR lamp P_{IR}, while the outputs are selected to be the average moisture content and the temperature, which are assumed to be measured via proper sensors (e.g. IR camera and nuclear magnetic resonance (NMR) moisture sensor). Γ is the average operator which can be defined as $\Gamma = (1/n)[1, \ldots, 1]_{1\times n}$ in the presence of n-node spatial discretization.

The UKF estimation is conducted based on this reduced-order nonlinear state-space model with the temporal coefficients as the states. These coefficients are estimated by the UKF from available online measurements of temperature and average moisture content. Then, the spatially distributed moisture content is reconstructed from POD approximation equation (24), which can then be used in the predictive control scheme described below.

NMPC for drying process

The main idea of MPC is to use an explicit plant model to predict system behaviour in a prediction horizon. Within the prediction horizon, an optimal open-loop input sequence can be generated to satisfy desired optimization criteria and the constraints of the process. Only the first input in this optimal sequence is often applied to the actual plant. Then, with the new available system states (obtained via the UKF reconstruction), the process is repeated using a receding prediction horizon.

For the drying problem, the remaining issue in formulating MPC is to define proper objective functions such that the control input (infrared power) is optimized. Three different objective functions regarding moisture content, paint quality and energy consumption are considered as follows

$$J(k) = J_A(k) + J_B(k) + J_C(k) \quad (28)$$

where

$$J_A(k) = \sum_{i=1}^{H_p} \alpha_i \left(\frac{\bar{\mathcal{M}}(k+i) - \bar{\mathcal{M}}_{ref}(k+i)}{\mathcal{M}_{ini}}\right)^2 \quad (29)$$

is the first objective function imposed to track a desired average moisture distribution $\bar{\mathcal{M}}_{ref}(t)$ during the drying process. $\mathcal{M}_{ini}$ is the known initial moisture content and H_p is the length of prediction horizon. In addition to moisture content, quality property is another important drying objective. As pointed out in Allanic et al.,[59] surface deterioration is usually due to early surface drying in the first drying stage, which has to be mitigated if possible. To address this problem, a second objective function related to film quality is selected to be

$$J_B(k) = \max_i \left\{\beta_i (\dot{\mathcal{M}}_s(k+i))^2\right\} \quad (i = 1, \ldots, H_p) \quad (30)$$

$\mathcal{M}_s$ stands for the surface moisture content. Due to the energy-intensive nature of the paint drying process,[66] energy consumption should also be considered as a control objective. A suitable form to penalize energy consumption is

$$J_C(k) = \sum_{i=1}^{H_p} \gamma_i \left(\frac{P_{IR}(k+i)}{P_{max}}\right)^2 \quad (31)$$

α_i, β_i and γ_i are weighted coefficients.

The final form of the constrained optimization problem for infrared drying can be formulated as

$$\min_{U(k)} J(k) \quad (32)$$

Subject to the constraints

$$\left[\left(\rho_p C_p z_p + \rho_s C_s z_s\right)\frac{dT}{dt} = P_{ab} - P_l - P_{ra} - P_{co}\right]_{\mathcal{D}}$$

$$\left[\dot{a}_j = \left(\varphi_j \frac{-\dot{m}(\mathcal{M},T)}{\rho_d}\right)\Big|_{\xi_d} - \int_0^{\xi_d} D\left(\sum_{k=1}^{L} a_k\varphi_k, T\right)\cdot\frac{\partial\sum_{k=1}^{L} a_k\varphi_k}{\partial\xi}\cdot\frac{d\varphi_j}{d\xi}\,d\xi\right]_{\mathcal{D}}$$

$$0 \leqslant P_{IR}(k+i) \leqslant P_{max},\ -\Delta P_{max} \leqslant \nabla P_{IR}(k+i) \leqslant \Delta P_{max},\quad i = 1,\ldots,H_p; j = 1,\ldots,L$$

where inputs $U(k) = [P_{IR}(k), \ldots, P_{IR}(k + H_p - 1)]^T$ and subscript $\mathcal{D}$ denotes the discretization in temporal domain. The last two inequalities are input constraints on the total power available and the rate of power change. They are subject to the physical limitations of the IR heat source used in the plant setup. The system states (moisture content) used in the objective functions are reconstructed from the temporal coefficients, which are estimated by the UKF. In other words, these temporal coefficients play an important role in linking the POD-Galerkin method, the UKF estimation and NMPC algorithm in the proposed scheme.

By solving the above optimization problem, an optimal input sequence U(k) is obtained. The first input in the sequence can be applied as the control input at time instant k, and the process is repeated.

Simulations

To verify the proposed model reduction, estimation and control strategies for the parabolic PDE system with nonlinear diffusion, simulations were conducted using the drying process model outlined above. The main control objective of this process is to track a predefined average moisture profile, which characterizes the typical desired drying profile of the paint material applied.

In order to apply the POD-Galerkin method for model reduction, an initial snapshot is required for POD analysis. However, due to practical sensing limitation, such a snapshot is often unavailable. To overcome this dilemma, multiple numerical simulations of the original PDE system are first conducted to generate the snapshot. These simulations are open loop with heat input intensity ranging from 2000 to 10,000 W/m^2. The distributed moisture content from these multiple simulations forms the initial snapshot for POD analysis. By applying the SVD method, the singular values are obtained as shown in Figure 3.

The first five POD basis functions, which correspond to the five largest singular values, are selected for model reduction with an accuracy of 99.9996%, according to equation (9).

To test the performance of the proposed UKF-based full state estimation, an open-loop simulation is first considered. Within this simulation scenario, the infrared heat input is set at 6000 W/m^2, and the only measureable outputs are the paint temperature and average moisture content. The UKF-based estimation works as follows: first, with the available measurements and the obtained POD basis functions, five time coefficients $a_l(k)$ $(l = 1, \ldots, 5)$ are estimated by the UKF-based estimation in equation (27). Then, the distributed moisture information is reconstructed by the POD approximation in equation (24). The simulation results are shown in Figures 4–7.

Figure 4 shows the simulated and estimated moisture content during the drying process. It can be seen that the estimated moisture content follows closely to the actual moisture content in open-loop simulation. The estimation errors, which include the POD approximation error and the POD-UKF combined estimation error, are demonstrated in Figures 5 and 6, respectively. It can be seen from these two figures that with a good initial snapshot (that covers most of the state-space) for POD basis generation, the POD approximation error is very small compared with the estimation error from UKF. To verify the boundedness of estimated temporal coefficients in the UKF estimation, Theorem 1 in Appendix 1 is applied. The boundedness condition on the nonlinear system of temporal coefficient (equation (27)) is checked and the norm of the

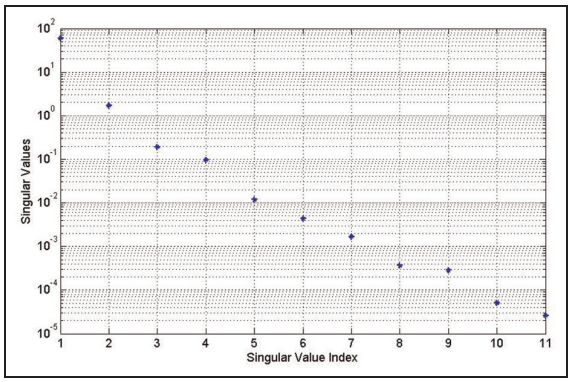

Figure 3. Singular values of snapshot.

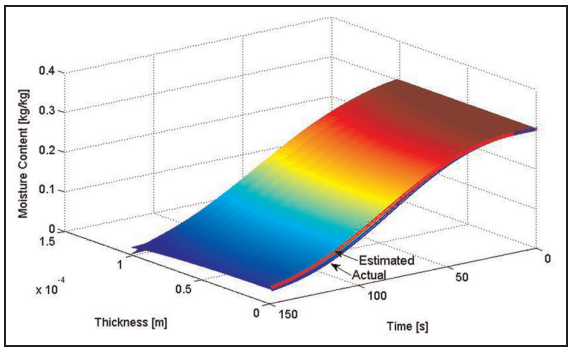

Figure 4. Actual and estimated moisture content.

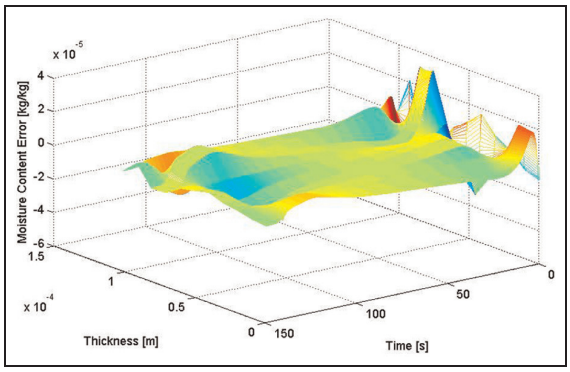

Figure 5. POD-approximated moisture error.

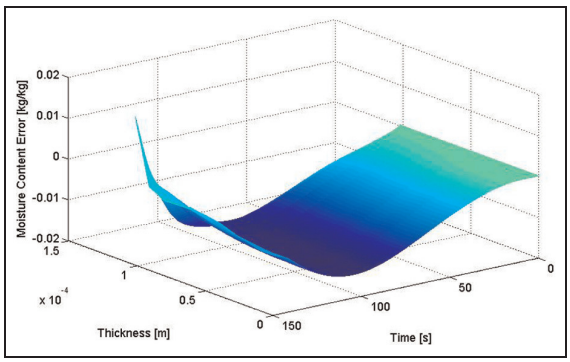

Figure 6. POD-UKF combined moisture estimation error.

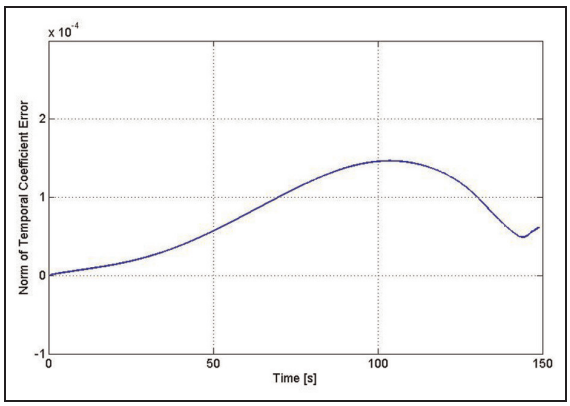

Figure 7. Norm of temporal coefficient estimation error.

estimated error of temporal coefficients is plotted in Figure 7. This is actually the size of the error vector (with dimension 5) showing the deviation between the estimated temporal coefficients and the simulated temporal coefficients from POD analysis. As we can see, the estimated error stays bounded within a very small range in the whole process. This results in the satisfactory performance of distributed moisture estimation as shown in Figure 4. Although the estimation error from

Table 1. Simulation conditions for the drying process.

Process parameters			
Initial moisture content	$\mathcal{M}_{ini}$	0.3	kg/kg
Initial coating temperature	T_b	293	K
Convective air temperature	T_{air}	325	K
Maximum input	P_{max}	10,000	W/m^2
Maximum input variation	Δ_{max}	1000	W/m^2
Simulation parameters			
Simulation time	t	140	s
Sample time	t_s	1	s
NMPC prediction horizon	H_p	8	1
Parameters in objectives	α_i	5×10^5	1
	β_i	9×10^3	s^2
	γ_i	4×10^4	1

NMPC: nonlinear model predictive control.

the POD approximation is relatively small given a good snapshot of the system, to improve the estimation performance further, one could update the POD basis online at selected intervals if a spatially distributed moisture measurement is available. However, the lack of such sensors is the difficulty that necessitates the need for estimation in the first place.

Based on the five POD basis functions selected and the acceptable UKF estimation performance for the open-loop process, we now look at the closed-loop estimation and control performance of the proposed NMPC scheme. Two closed-loop simulations were conducted. In the first one, the distributed moisture content is assumed measureable and used directly in online optimization of the MPC. This scenario is admittedly not practical and is therefore used only as a benchmark. In the second simulation, the UKF is applied to estimate the temporal POD coefficients online from the available measurements (temperature and average moisture) and then subsequently reconstructing the moisture distribution approximately. The initial infrared heat input is 5000 W/m^2. With the available POD basis functions and uniform distributed initial moisture content set to 0.3 kg/kg, the initial temporal coefficient can be readily derived. Moreover, initial state covariance is set to be zero in the UKF estimation. The covariance matrix of output/measurement noise is assumed to be very small (10^{-6}). The reference moisture content trajectory was generated from off-line simulations of the drying plant model (coupled PDE-ODE) with a constant heat input at 6000 W/m^2. This ensures that the so-obtained desired trajectory is feasible. Other simulation conditions are provided in Table 1.

The weighting coefficients in the objective function offer the flexibility to assign emphasis on different process objectives for the controller. Early surface drying and energy usage could be improved with relatively large coefficients for quality and energy consumption. However, this comes with the degradation of average moisture tracking performance. In fact, there is always a trade-off between average moisture content tracking performance and quality/energy considerations. In this

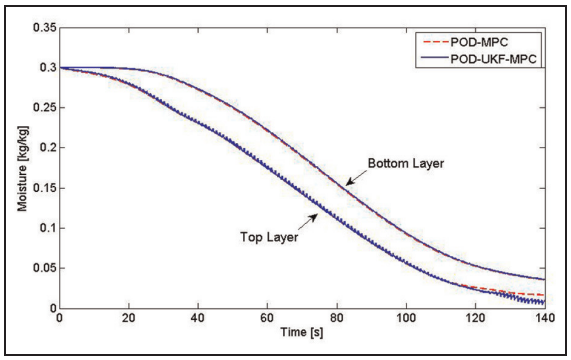

Figure 8. Top and bottom moisture content.

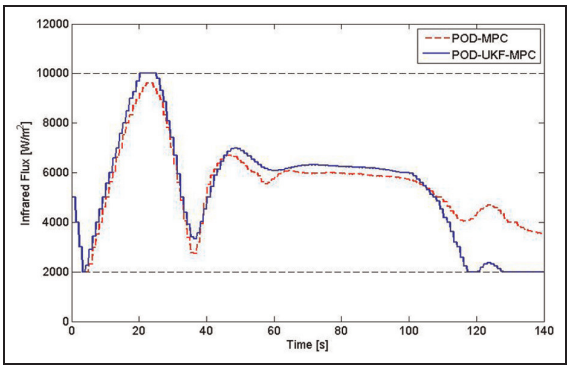

Figure 10. Infrared flux.

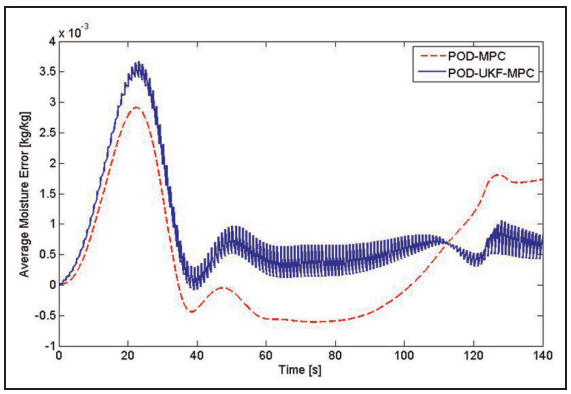

Figure 9. Average moisture error.

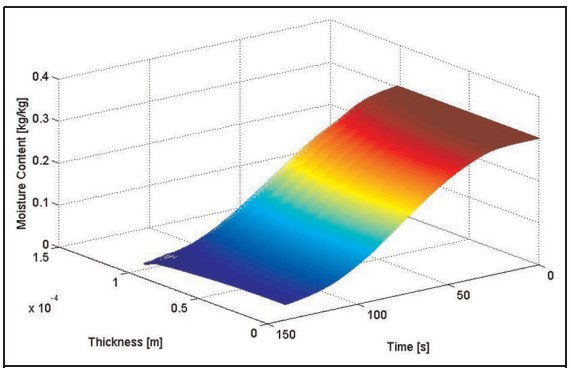

Figure 11. Moisture content with UKF estimation.

article, we adopted these coefficients as provided in Table 1. Further discussion about these coefficients can be found in our previous work.[67]

In this article, the proposed optimization problem with nonlinear constraints in the NMPC framework is solved by the sequential quadratic programming (SQP) method implemented in MATLAB. For the definition of objective functions and other simulation parameters in the drying process, feasible solutions exist in our simulation studies. However, we note that feasibility for general nonlinear DPSs under the proposed scheme is not guaranteed. Related discussions on this topic can be found in Martinsen et al.[68] and Nagy et al.[69] The results of these two simulations are presented in Figures 8–12. In these simulations, the nonlinear PDE-ODE coupled model of the drying processes serves as the plant.

Moisture content at the top and bottom of the paint film is shown in Figure 8. It can be seen that asymmetric evaporation (only from the top surface) and diffusion within the paint lead to the unevenly distributed moisture content. However, the top (bottom) moisture content profiles in these two simulations show good agreement with each other, which validates the UKF-based estimation. The tracking error of average moisture content is shown in Figure 9. As can be seen,

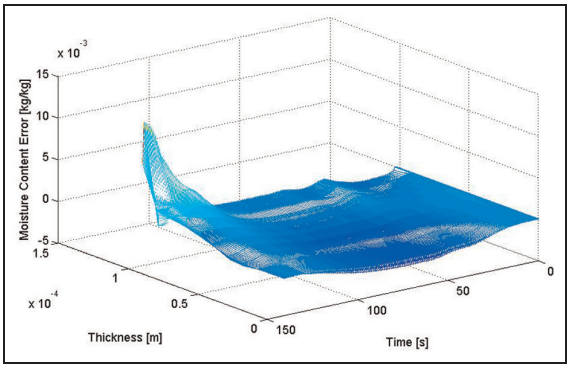

Figure 12. Moisture content error during process.

tracking errors in both of these two simulations stay in a small range during the drying process. This helps to achieve a good average moisture tracking performance with the proposed control scheme. Meanwhile, it is observed that small chattering shows up on the error profile of POD-UKF-MPC scheme. This is mainly due to the existence of the measurement noise assumed in the UKF-based estimation. Although the two profiles of tracking error share the same shape in most of the drying process, slight performance degradation in terms of error magnitude can be observed in the

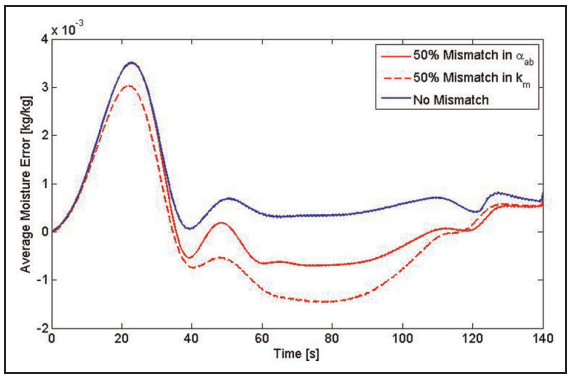

Figure 13. Average moisture error with parameter mismatch.

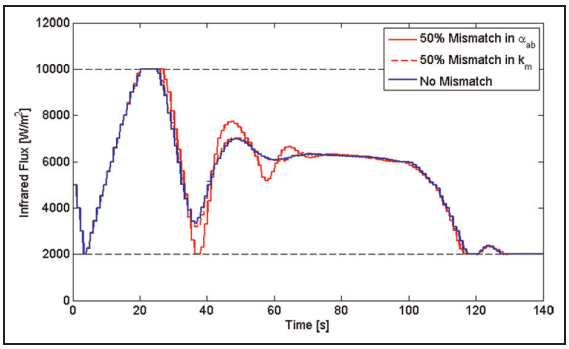

Figure 14. Infrared flux with parameter mismatch.

simulation with the UKF. Moreover, a relatively big difference of tracking error is shown at the end of the drying process. This performance deviation can be explained by the relatively large estimation error (compared with actual moisture content) at the end from the UKF estimation, which is absent in the ideal POD-MPC case as measurements are assumed available. Figure 10 shows the comparison of infrared heat inputs for these two simulation scenarios. It is clear that at the beginning, with the selected quality objective, control input is lowered to prevent large surface drying rate and at the end of drying, the heat input is also lowered to minimize the energy consumption. The evolution of UKF estimated moisture content during the process is illustrated in Figure 11. For a comparison, the difference of distributed moisture content between these two simulation sets is shown in Figure 12.

The above simulation results demonstrate that the proposed UKF-based POD-NMPC scheme is able to control the infrared drying process with the selected optimization objectives. Although a small degradation exists with the UKF estimation as the process evolves, the overall control performance of the proposed scheme is satisfactory under practical sensing considerations (versus unrealistically assuming the full distributed state measurement is available).

To explore the potential robustness of the proposed scheme, we also conducted a few robustness tests by perturbing some parameters in the diffusion and temperature equations of the plant (e.g. by as much as 50% perturbation for the absorption coefficient α_{ab} and the mass transfer coefficient k_m) while keeping the nominal controller and estimator designs. The resultant average moisture error and infrared heat input are illustrated in Figures 13 and 14.

It can be seen from Figures 13 and 14 that with parameter mismatch in either the diffusion or the heat equations, the control performance in terms of the average moisture error deviates from that in the nominal case. Moreover, with the same amount of mismatch, performance of the proposed scheme is more affected by the perturbation in the mass transfer coefficient k_m than that in the absorption coefficient α_{ab}. This is possibly due to the fact that the drying process is actually a diffusion-dominated process and the mass transfer coefficient mainly controls the diffusion rate on the top surface. Despite of slight deviations from the results in the nominal case, the average moisture is still controlled with relatively small tracking errors. This shows good robustness of the proposed control and estimation scheme for the considered cases. However, for a more rigorous proof, robust NMPC formulations need to be pursued. Examples include robust NMPC that solves an open-loop min–max problem considering the worst case of mismatch[70] or the H_∞ NMPC, where the standard H_∞ problem is solved in a receding horizon.[71]

Remark 1. The relative dynamics of the estimator and controller have practical implications. In a typical modern personal laptop, the NMPC computation time observed in the simulations was of the order of 0.5 s. The dynamics of the diffusion-based DPSs are usually very slow (e.g. time constant of the drying process is around 90 s following the definition in Maroulis and Saravacos[72]). So, with selected prediction horizon, the control update loop is sufficiently fast. On the other hand, the UKF estimation typically converges fast and the computational time is around 6.5 ms. Furthermore, these slow plant, faster NMPC and even much faster estimator dynamics allow ready use of typical sensors for temperature (IR camera, response time order of a millisecond) and average moisture (NMR sensor, much faster) for real-time implementation of the proposed approach.

Conclusion

This article proposed and demonstrated a UKF-based state estimation and control scheme for the processes described by parabolic PDEs with nonlinear diffusivity. The basic idea of the method is first to obtain a set of problem-oriented basis functions using POD. This set of optimal basis functions captures the dominant system dynamics in the spatial domain. Then, Galerkin projection method is applied to derive a ROM (set of nonlinear ODEs) in terms of the dynamics of the

temporal coefficients in POD approximation. To overcome the lack of suitable sensing for distributed measurements, the UKF is used to estimate the temporal coefficients in order to subsequently reconstruct full system states. Finally, NMPC scheme is implemented with the optimization criteria such as profile tracking and energy consumption. To validate the proposed control scheme, infrared drying process of waterborne coatings is used as an example. Simulation results demonstrated the application of proposed estimation and control method.

There are some important issues that need further research. To the best of our knowledge, there is no complete work on the stability analysis of closed-loop UKF-NMPC schemes. In Huang et al.,[73] a stability analysis is outlined for the EKF-NMPC scheme and input to state practical stability (ISpS) is proved for the closed-loop system. However, such stability is achieved under certain assumptions such as the boundedness of linearized system matrix, which only exists in the EKF formulation. It seems possible to analyse the closed-loop stability of UKF-NMPC scheme along similar lines by keeping the nonlinear transformation in UKF. This is a possible further research direction. Moreover, the rigorous formulation of a robust version of the proposed UKF-NMPC scheme for PDEs with nonlinear diffusivity is a second further research topic.

Declaration of conflicting interests

The authors declare that there is no conflict of interest.

Funding

This work was financially supported, in part, by the US National Science Foundation under NSF Grant No. CMMI-1055254 and the US DOE Graduate Automotive Technology Education Program under grant no. DE-EE0005571.

References

1. Ray WH. *Advanced process control*. New York: McGraw-Hill, 1981.
2. Padhi R and Ali SF. An account of chronological developments in control of distributed parameter systems. *Annu Rev Control* 2009; 33(1): 59–68.
3. Li H. *Spatio-temporal modeling of nonlinear distributed parameter systems*. New York: Springer, 2011.
4. Butkovskii AG. *Green's functions and transfer functions handbook*. New York: Halsted Press, 1982.
5. Fletcher CA. *Computational Galerkin methods*. New York: Springer, 1984.
6. Temam R. *Infinite-dimensional dynamical systems in mechanics and physics*. New York: Springer, 1988.
7. Baker J and Christofides PD. Finite-dimensional approximation and control of non-linear parabolic PDE systems. *Int J Control* 2000; 73(5): 439–456.
8. Armaou A and Christofides PD. Finite-dimensional control of nonlinear parabolic PDE systems with time-dependent spatial domains using empirical eigenfunctions. *Appl Math Comput Sci* 2001; 11(2): 287–318.
9. Foias C, Sell GR and Temam R. Inertial manifolds for nonlinear evolutionary equations. *J Differ Equations* 1988; 73(2): 309–353.
10. Foias C, Sell GR and Titi ES. Exponential tracking and approximation of inertial manifolds for dissipative nonlinear equations. *J Dyn Differ Equ* 1989; 1(2): 199–244.
11. Christofides PD and Daoutidis P. Finite-dimensional control of parabolic PDE systems using approximate inertial manifolds. In: *Proceedings of the 36th IEEE conference on decision and control*, San Diego, CA, 10–12 December 1997, pp.1068–1073. New York: IEEE.
12. Titi ES. On approximate inertial manifolds to the Navier–Stokes equations. *J Math Anal Appl* 1990; 149(2): 540–557.
13. Deng H, Li H-X and Chen G. Spectral-approximation-based intelligent modeling for distributed thermal processes. *IEEE T Contr Syst T* 2005; 13(5): 686–700.
14. Dufour P, Touré Y, Blanc D, et al. On nonlinear distributed parameter model predictive control strategy: on-line calculation time reduction and application to an experimental drying process. *Comput Chem Eng* 2003; 27(11): 1533–1542.
15. Dufour P, Touré Y, Michaud DJ, et al. Optimal trajectory determination and tracking of an autoclave curing process: a model based approach. In: *Proceedings of the 5th IFAC-IEEE European control conference (ECC)*, Karlsruhe, Germany, 31 August–3 September 1999.
16. Pinnau R. Model reduction via proper orthogonal decomposition. *Math Indust* 2008; 13: 95–109.
17. Luchtenburg D, Noack B and Schlegel M. *An introduction to the POD Galerkin method for fluid flows with analytical examples and MATLAB source codes*. Technical report 01/2009, August 2009. Berlin: Berlin Institute of Technology.
18. Kunisch K and Volkwein S. Galerkin proper orthogonal decomposition methods for parabolic problems. *Numer Math* 2001; 90(1): 117–148.
19. Kunisch K and Volkwein S. Galerkin proper orthogonal decomposition methods for a general equation in fluid dynamics. *SIAM J Numer Anal* 2002; 40(2): 492–515.
20. John T, Guay M, Hariharan N, et al. POD-based observer for estimation in Navier–Stokes flow. *Comput Chem Eng* 2010; 34(6): 965–975.
21. Alonso AA, Kevrekidis IG, Banga JR, et al. Optimal sensor location and reduced order observer design for distributed process systems. *Comput Chem Eng* 2004; 28(1): 27–35.
22. Shvartsman SY, Theodoropoulos C, Rico-Martínez R, et al. Order reduction for nonlinear dynamic models of distributed reacting systems. *J Process Contr* 2000; 10(2–3): 177–184.
23. Krstic M and Smyshlyaev A. *Boundary control of PDEs: a course on backstepping designs*. Philadelphia, PA: SIAM, 2008.
24. Xu C, Ou Y and Schuster E. POD-based reduced order optimal control of parabolic PDE systems via diffusivity-interior-boundary actuation. In: *46th IEEE conference on decision and control*, New Orleans, LA, 12–14 December 2007, pp.3519–3524. New York: IEEE.
25. Xu C, Ou Y and Schuster E. Sequential linear quadratic control of bilinear parabolic PDEs based on POD model reduction. *Automatica* 2011; 47(2): 418–426.

26. Fernandez-Camacho E and Bordons-Alba C. *Model predictive control in the process industry*. New York: Springer, 1995.
27. Dufour P, Laurent P and Xu CZ. Model predictive control of the water based painting drying using a humidity profile soft sensor and a temperature measurement. In: *Proceedings of the 14th international drying symposium (IDS)*, São Paulo, Brazil, 22–25 August 2004. São Paulo, Brazil: UNICAMP.
28. Abukhalifeh H, Dhib R and Fayed M. Model predictive control of an infrared-convective dryer. *Dry Technol* 2005; 23(3): 497–511.
29. Padhiyar N and Bhartiya S. Profile control in distributed parameter systems using lexicographic optimization based MPC. *J Process Contr* 2009; 19(1): 100–109.
30. Vada J, Slupphaug O, Johansen TA, et al. Linear MPC with optimal prioritized infeasibility handling: application, computational issues and stability. *Automatica* 2001; 37(11): 1835–1843.
31. Dufour P, Blanc D, Touré Y, et al. Infrared drying process of an experimental water painting: model predictive control. *Dry Technol* 2004; 22(1–2): 269–284.
32. Larabi MC, Dufour P, Laurent P, et al. Predictive control of a nonlinear distributed parameter system: real time control of a painting film drying process. In: *Proceedings of the 14th mathematical theory on network and systems (MTNS)*, Perpignan, France, 19–23 June 2000.
33. Xie W, Bonis I and Theodoropoulos C. Off-line model reduction for on-line linear MPC of nonlinear large-scale distributed systems. *Comput Chem Eng* 2011; 35(5): 750–757.
34. Dubljevic S, El-Farra NH, Mhaskar P, et al. Predictive control of parabolic PDEs with state and control constraints. *Int J Robust Nonlin* 2006; 16(16): 749–772.
35. García MR, Vilas C, Santos LO, et al. A robust multimodel predictive controller for distributed parameter systems. *J Process Contr* 2012; 22(1): 60–71.
36. Li M and Christofides PD. Optimal control of diffusion-convection-reaction processes using reduced-order models. *Comput Chem Eng* 2008; 32(9): 2123–2135.
37. De Battista H, Picó J, Garelli F, et al. Reaction rate reconstruction from biomass concentration measurement in bioreactors using modified second-order sliding mode algorithms. *Bioproc Biosyst Eng* 2012; 35(9): 1615–1625.
38. MacKunis W, Drakunov S, Reyhanoglu M, et al. Nonlinear estimation of fluid flow velocity fields. In: *50th IEEE conference on decision and control and European control conference (CDC-ECC)*, Orlando, FL, 12–15 December 2011, pp.6931–6935. New York: IEEE.
39. Hidayat Z, Babuska R, De Schutter B, et al. Observers for linear distributed-parameter systems: a survey. In: *IEEE international symposium on robotic and sensors environments (ROSE)*, Montreal, QC, Canada, 17–18 September 2011, pp.166–171. New York: IEEE.
40. Jazwinski AH. *Stochastic processes and filtering theory*. New York: Dover Publications, 2007.
41. Julier SJ, Uhlmann JK and Durrant-Whyte HF. A new approach for filtering nonlinear systems. In: *Proceedings of the 1995 American control conference*, Seattle, WA, 21–23 June 1995, pp.1628–1632. New York: IEEE.
42. Julier SJ and Uhlmann JK. *A general method for approximating nonlinear transformations of probability distributions* (technical report). Oxford: Robotics Research Group, Department of Engineering Science, University of Oxford, 1996.
43. Julier S, Uhlmann J and Durrant-Whyte HF. A new method for the nonlinear transformation of means and covariances in filters and estimators. *IEEE T Automat Contr* 2000; 45(3): 477–482.
44. Xiong K, Chan C and Zhang H. Detection of satellite attitude sensor faults using the UKF. *IEEE T Aero Elec Sys* 2007; 43(2): 480–491.
45. Kandepu R, Foss B and Imsland L. Applying the unscented Kalman filter for nonlinear state estimation. *J Process Contr* 2008; 18(7): 753–768.
46. Ristic B, Farina A, Benvenuti D, et al. Performance bounds and comparison of nonlinear filters for tracking a ballistic object on re-entry. *IEE Proc F* 2003; 150: 65–70.
47. Xiong K, Liu L and Zhang H. Modified unscented Kalman filtering and its application in autonomous satellite navigation. *Aerosp Sci Technol* 2009; 13(4): 238–246.
48. Julier SJ and Uhlmann JK. A new extension of the Kalman filter to nonlinear systems. In: *Proceedings of SPIE aerosense'97*, Orlando, FL, 21–25 April 1997, pp.182–193. Bellingham, WA: SPIE.
49. Wan EA and Van der Merwe R. The unscented Kalman filter for nonlinear estimation. In: *The IEEE 2000. Adaptive systems for signal processing, communications, and control symposium (AS-SPCC)*, Lake Louise, AB, Canada, 1–4 October 2000, pp.153–158. New York: IEEE.
50. Christofides PD. *Nonlinear and robust control of PDE systems: methods and applications to transport-reaction problems*. New York: Springer, 2001.
51. El-Farra NH, Armaou A and Christofides PD. Analysis and control of parabolic PDE systems with input constraints. *Automatica* 2003; 39(4): 715–725.
52. Lumley J. The structure of inhomogeneous turbulent flows. In: Yaglom AM and Tatarsky VI (eds) *Atmospheric turbulence and radio wave propagation*. Moscow: Nauka, 1967, pp.166–178.
53. Sirovich L. Turbulence and the dynamics of coherent structures. I – Coherent structures. II – Symmetries and transformations. III – Dynamics and scaling. *Q Appl Math* 1987; 45: 561–571.
54. Wu C, Liang Y, Lin W, et al. A note on equivalence of proper orthogonal decomposition methods. *J Sound Vib* 2003; 265: 1103–1110.
55. Shidfar A and Mohammadi M. Using empirical Eigenfunctions and Galerkin method to two-phase transport models. *Numer Meth Part D E* 2007; 23(2): 456–474.
56. Kunisch K and Volkwein S. Control of the Burgers equation by a reduced-order approach using proper orthogonal decomposition. *J Optimiz Theory App* 1999; 102(2): 345–371.
57. Xiong K, Zhang H and Chan C. Performance evaluation of UKF-based nonlinear filtering. *Automatica* 2006; 42(2): 261–270.
58. E Source Companies, LLC. *Curing and drying operations: the pros and cons of infrared heating*, 2005, https://www.we-energies.com/business/energyeff/curingdrying.pdf
59. Allanic N, Salagnac P and Glouannec P. Optimal constrained control of an infrared-convective drying of a polymer aqueous solution. *Chem Eng Res Des* 2009; 87(7): 908–914.

60. Allanic N, Salagnac P, Glouannec P, et al. Estimation of an effective water diffusion coefficient during infrared-convective drying of a polymer solution. *AICHE J* 2009; 55(9): 2345–2355.
61. Brinckmann F, Lehnhäuser T, Löffler R, et al. Simulation of the heat and mass transfer during paint drying processes. In: *ANSYS conference and 27th CADFEM users' meeting*, Leipzig, Germany, 18–20 November 2009.
62. Domnick J, Gruseck D, Pulli K, et al. Investigations of the drying process of a water based paint film for automotive applications. *Chem Eng Process* 2011; 50(5–6): 495–502.
63. Crank J. *The mathematics of diffusion*. Oxford: Oxford University Press, 1979.
64. Ruiz-Cabrera M, Foucat L, Bonny J, et al. Assessment of water diffusivity in gelatine gel from moisture profiles. II. Data processing adapted to material shrinkage. *J Food Eng* 2005; 68(2): 221–231.
65. Blanc D, Vessot S, Laurent P, et al. Study and modelling of coated car painting film by infrared or convective drying. *Dry Technol* 1997; 15(9): 2303–2323.
66. Omar MA. *The automotive body manufacturing systems and processes*. Chichester: John Wiley & Sons, 2011.
67. Cao X and Ayalew B. POD-Galerkin-reduced model predictive control for radiative drying of coatings. In: *ASME 2013. Dynamic systems and control conference*, Palo Alto, CA, 21–23 October 2013. New York: American Society of Mechanical Engineers (ASME).
68. Martinsen F, Biegler LT and Foss BA. A new optimization algorithm with application to nonlinear MPC. *J Process Contr* 2004; 14(8): 853–865.
69. Nagy Z, Findeisen R, Diehl M, et al. Real-time feasibility of nonlinear predictive control for large scale processes-a case study. In: *Proceedings of the 2000 American control conference*, Chicago, IL, 28–30 June 2000, pp.4249–4253. New York: IEEE.
70. Limón D, Alamo T, Salas F, et al. Input to state stability of min-max MPC controllers for nonlinear systems with bounded uncertainties. *Automatica* 2006; 42(5): 797–803.
71. Magni L, Nijmeijer H and Van Der Schaft A. A receding-horizon approach to the nonlinear H_∞ control problem. *Automatica* 2001; 37(3): 429–435.
72. Maroulis ZB and Saravacos GD. *Food process design*. Boca Raton, FL: CRC Press, 2003.
73. Huang R, Patwardhan SC and Biegler LT. Robust stability of nonlinear model predictive control based on extended Kalman filter. *J Process Contr* 2012; 22(1): 82–89.

Appendix 1

Sufficient condition for unscented Kalman filter stability

Although the unscented Kalman filter (UKF) is gaining popularity, there are few stability analyses for it under various restrictive assumptions. Encouraged by the established boundedness analysis for the extended Kalman filter (EKF), Xiong et al.[44,57] proposed a sufficient condition to ensure the boundedness of the UKF estimation error. This sufficient condition, although rigorous, is still implicit because of the use of an unknown instrumental diagonal matrix. In this section, a set of more straightforward sufficient condition for the UKF stability are proposed building on the results in Xiong et al.[57]

Theorem 1. For a nonlinear stochastic system (16) with linear output (17) under the UKF steps summarized above, if the following conditions hold:

1. Posteriori error $\tilde{x}_{k-1} = x_{k-1} - \hat{x}_{k-1}$ and covariance matrix $\hat{P}_{k-1}$ are bounded;
2. Covariance matrices for process and output noises as well as the predicted covariance are bounded with constants q_{max}, r_{min}, p_{max} and p_{min}

$$Q_k \leqslant q_{max} I$$
$$R_k \geqslant r_{min} I$$
$$p_{min} I \leqslant \hat{P}_{k|k-1} \leqslant p_{max} I$$

3. The nonlinear system satisfies

$$f^1_{min}{}^2 I \leqslant F^1_k F^{1\,T}_k \leqslant f^1_{max}{}^2 I$$
$$f^2_{min}{}^2 I \leqslant F^2_k F^{2\,T}_k \leqslant f^2_{max}{}^2 I$$
$$h_{min}{}^2 I \leqslant H_k H_k{}^T \leqslant h_{max}{}^2 I$$

with constants f^1_{min}, f^1_{max}, f^2_{min}, f^2_{max}, h_{min}, h_{max} and $F^1_k = \partial \mathcal{F}/\partial x|_{x=\hat{x}_{k-1}}$, $F^2_k = \partial^2 \mathcal{F}/\partial x^2|_{x=\hat{x}_{k-1}}$. Then, the estimation error $\tilde{x}_k = x_k - \hat{x}_k$ is bounded in the mean square sense.[57]

This proposed sufficient condition is mainly based on the assumption that the first and second derivatives of the system nonlinearity are bounded. With further constraints on system noises and initial estimates, the stability can be analysed recursively.

Proof. Applying Taylor expansion to the discretized state, we have

$$x_k = \mathcal{F}(\hat{x}_{k-1} + \tilde{x}_{k-1}) = \mathcal{F}(\hat{x}_{k-1}) + \mathcal{F}'(\hat{x}_{k-1})\tilde{x}_{k-1} + R_1$$

where R_1 is the truncation error and is equal to

$$R_1 = \frac{\mathcal{F}^{(2)}(\xi)}{2}\tilde{x}^2_{k-1}, \quad \xi \in (\hat{x}_{k-1}, x_k)$$

Similarly, for $\hat{x}_{k|k-1}$

$$\hat{x}_{k|k-1} = \varpi_0 \mathcal{F}(\hat{x}_{k-1}) + \varpi_i \sum_{i=1}^{n} \mathcal{F}(\hat{x}_{k-1} + \sigma_i) + \varpi_{i+n} \sum_{i=1}^{n} \mathcal{F}(\hat{x}_{k-1} - \sigma_i)$$

we have the results

$$\sum_{i=1}^{n} \mathcal{F}(\hat{x}_{k-1} + \sigma_i) = \sum_{i=1}^{n} [\mathcal{F}(\hat{x}_{k-1}) + \mathcal{F}'(\hat{x}_{k-1})\sigma_i + R_{1i}]$$

where

$$R_{1i} = \frac{\mathcal{F}^{(2)}(\varepsilon_1)}{2}\sigma_i^2, \quad \varepsilon_1 \in (\hat{x}_{k-1}, \hat{x}_{k-1} + \sigma_i)$$

and

$$\sum_{i=1}^{n} \mathcal{F}(\hat{x}_{k-1} - \sigma_i) = \sum_{i=1}^{n} [\mathcal{F}(\hat{x}_{k-1}) - \mathcal{F}'(\hat{x}_{k-1})\sigma_i + R_{2i}]$$

where

$$R_{2i} = \frac{\mathcal{F}^{(2)}(\varepsilon_2)}{2}\sigma_i^2, \quad \varepsilon_2 \in (\hat{x}_{k-1} - \sigma_i, \hat{x}_{k-1})$$

Finally, we have

$$\begin{aligned}\hat{x}_{k|k-1} &= \mathcal{F}(\hat{x}_{k-1})\left[\varpi_0 + \sum_{i=1}^{n}(\varpi_i + \varpi_{i+n})\right] \\ &\quad + \sum_{i=1}^{n} \varpi_i R_{1i} + \sum_{i=1}^{n} \varpi_{i+n} R_{2i} \\ &= \mathcal{F}(\hat{x}_{k-1}) + \sum_{i=1}^{n} \varpi_i (R_{1i} + R_{2i})\end{aligned}$$

Then, the prior error can be written as

$$\begin{aligned}\tilde{x}_{k|k-1} &= x_k - \hat{x}_{k|k-1} \\ &= \mathcal{F}(\hat{x}_{k-1}) + \mathcal{F}'(\hat{x}_{k-1})\tilde{x}_{k-1} \\ &\quad + R_1 - \left[\mathcal{F}(\hat{x}_{k-1}) + \sum_{i=1}^{n} \varpi_i (R_{1i} + R_{2i})\right] \\ &= \mathcal{F}'(\hat{x}_{k-1})\tilde{x}_{k-1} + R_1 - \sum_{i=1}^{n} \varpi_i (R_{1i} + R_{2i}) \\ &= F_k^1 \tilde{x}_{k-1} + R_1 - \sum_{i=1}^{n} \varpi_i (R_{1i} + R_{2i}) \\ &= \beta_k F_k^1 \tilde{x}_{k-1} \qquad (33)\end{aligned}$$

From the above equation, if the assumption (3) in Theorem 1 holds, R_1, R_{1i} and R_{2i} are bounded. Combined with the assumption that posterior error $\tilde{x}_{k-1}$ is bounded, it is clear that unknown instrumental diagonal matrix β_k is also bounded for equation (33). Furthermore, with the condition of bounded predictive covariance $\hat{P}_{k|k-1}$, the other two sufficient conditions related to corrected covariance $\hat{P}_k$ and intermediate variable $\hat{Q}_k = \hat{P}_{k|k-1} - \beta_k F_k^1 \hat{P}_{k-1} F_k^{1T} \beta_k$ are also bounded. Then, following on the rest of the stability analysis given in Xiong et al.,[57] it can be shown that the estimation error of UKF is bounded in mean square.